Toward Tailorable Porous Organic Polymer Networks: A High-Temperature Dynamic Polymerization Scheme Based on Aromatic Nitriles

Pierre Kuhn,* Arne Thomas, and Markus Antonietti

Max Planck Institute of Colloids and Interfaces, Department of Colloid Chemistry, Research Campus Golm, 14424 Potsdam, Germany

Received October 15, 2008; Revised Manuscript Received November 20, 2008

ABSTRACT: Triazine-based polymer scaffolds with controllable porosity were prepared through a dynamic polymerization scheme based on a broad variety of aromatic nitriles, upon polytrimerization of the latter from $ZnCl_2$ salt melts at high temperatures. In the present study, the reaction parameters such as the temperature and monomer concentration as well as the geometry and functionality of the monomers were systematically varied. A comprehensive overview of the influences of these parameters on the outcome of the polymerization reaction in terms of chemical nature and porous properties of the materials is proposed. Rather than the variation of the monomer size and/or geometry, the reaction parameters were found to play a crucial role for tuning the porosity of the materials and especially the reaction temperature. Finally, the use of functional aromatic bridging units allowed the formation of functional polymer scaffolds with the ability to coordinate metal salts, introducing the possibility to design new metallo-organic materials.

Introduction

Micro- and mesoporous polymers are relevant, classical materials, with application as sorption materials or in chromatography.[1−5] Their interest has been revamped by the upcoming technological problems of the new energy cycles, thus stimulating research on "energy materials/polymers" necessary for the production of energy (e.g., novel catalysts and catalyst supports, fuel cell membranes), its storage (hydrogen, lithium, etc.), but also for green processes (wastewater treatment, detoxification, etc.). Controlled microporous materials were up to now however a domain of inorganic chemistry, as there are standard recipes for zeolites and activated carbon blacks.[6,7] Hybrid materials such as certain metal−organic frameworks (MOFs) and especially silicas of the MCM family extended those profiles to the mesopore range.[8,9] Despite the remarkable progress achieved by those systems, they present, as inorganic materials, serious restrictions such as glass-like brittleness, sensitivity against hot water, acids and bases, or limitations in the accessible chemical functionality.

Alternatively, the search for "all organic" porous materials made by polymerization processes of organic monomers can not only lead to enhanced performances (shapeability and simplified synthesis and processing) but also introduce new opportunities relying on functional properties, such as electronic conductivity or complex, converging functionalities. It is also the hope that these polymer-like materials may overpass the limitations of their counterparts in terms of pore size and connectivity. Therefore, it is no wonder that since a few years, more and more research groups became interested in the development of porous organic materials, and several different types of porous polymer networks have been synthesized.[10−17] Most of these examples introduced the chemical tools required to build such materials, through cross-linking strategies, reversible polymerization systems for crystalline materials, and precise building blocks allowing the appearance of a stable porosity. On the other side, some studies already proved that porous polymeric materials can feature novel intrinsic structural properties.[15,16,18] All these materials were prepared following conventional synthetic approaches, i.e., by using well-known organic reactions in an organic solvent at low temperatures. However, very high porosities (surface area $\geq$2000−3000 m^2 g^{-1}, pore volume $\geq$2 cm^3 g^{-1}) are still the domain of MOFs and amorphous activated carbons. In our opinion, this is caused by the effects of cold flow and ductility of polymers, which close a majority of the very fine pores of those networks.[18]

Inspired by the chemistry of carbon nitrides, which can be prepared by a high-temperature polymerization process from cyanamide at 500 °C,[19−21] we were convinced that high-temperature condensation of stable organic moieties could lead to porous polymer scaffolds which combine very high porosities and functionalities in their well-defined structure. Here, we especially wanted to make use of dynamic reversibility of bond and structure formation, as this seems to be most appropriate to make regular structure formation to occur. This of course implies that it is possible to carry out organic polymerization reactions at high temperatures, i.e., that organic molecules can be reacted in a controlled way at high temperatures (contrary to the synthesis of activated carbons where a lot of reactions are occurring in an uncontrolled fashion). Aromatic molecules with special substitution patterns are well-known to be thermally stable at temperatures as high as 400−500 °C, and nitriles and oligonitriles are among them.[22] From the trimerization of aromatic nitriles through Lewis acid catalysis at temperatures of about 300−400 °C, triazines can be conveniently prepared.[23] This reaction is moreover reversible as the retro-trimerization is also occurring at these temperatures, thus opening the opportunities of dynamic self-optimization of the as formed network structure. Triazine-based systems would also lead to structurally stiff, all-aromatic polymer structures with very low bendability, favorable for the preservation of a stable microporosity. This is illustrated in Scheme 1.

A second key point of the current approach is the choice of the reaction medium. To develop and preserve porosity in a material, a porogen is required, being often simply the solvent itself. For performing reactions at the targeted temperatures, a high-temperature stable solvent has to be chosen. At these temperatures, inorganic salts can be reasonably envisaged, and zinc chloride turned out to be a good choice for several reasons. It is a smooth Lewis acid and therefore a catalyst for the

* Corresponding author. E-mail: kuhn@mpikg.mpg.de.

10.1021/ma802322j CCC: $40.75
Published on Web 12/09/2008

Scheme 1. Nitrile Trimerization of a Model Aromatic Nitrile Leading to an Idealized Stiff, Polycyclic Polymer Architecture

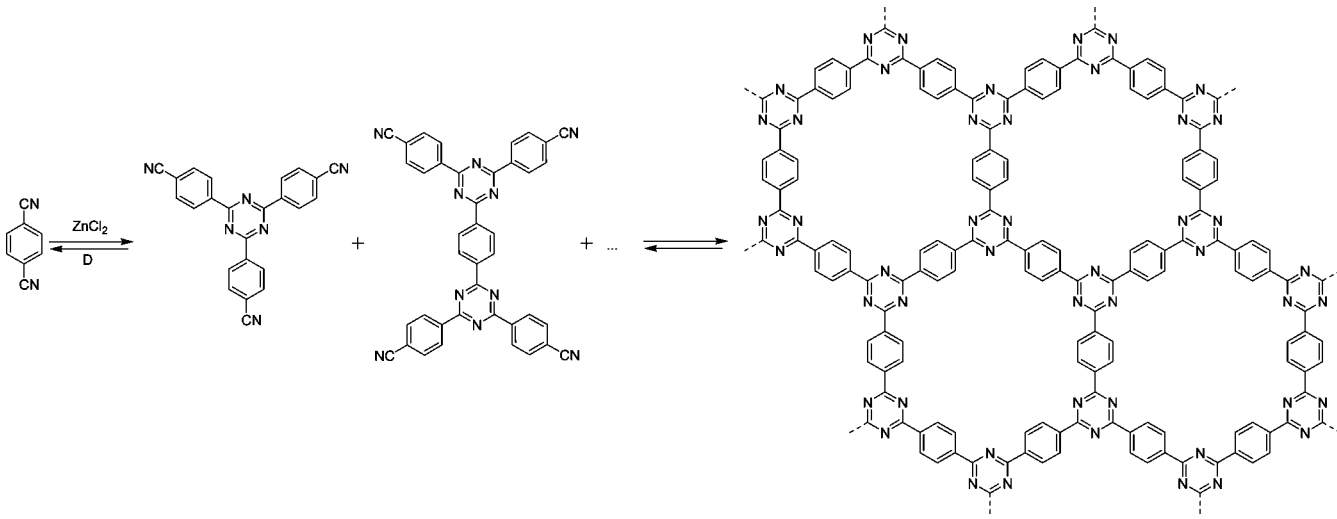

trimerization, it is liquid in the desired temperature range for the reaction (280−730 °C), and finally it is miscible in all proportions with all the nitriles listed below. This dynamic nitrile trimerization (DNT) system has recently been proven to be very efficient for the production of porous polymers scaffolds.[13,24] It is the purpose of this article to provide a more detailed study of this polymerization system, relating the properties of the as-formed polymer to the monomer architecture, its concentration, and to the reaction temperature, as subtle variations of these parameters can lead to very different scaffolded structures and in turn to a broad range of materials with different characteristics.

Experimental Part

Chemicals. Zinc chloride (ABCR, anhydrous, 98%) was stored in a glovebox and used as received. 1,4-Dicyanobenzene (pDCB), 1,3-dicyanobenzene (mDCB), 1,4-dicyanobenzene (oDCB), 1,3,5-tricyanobenzene (TCB), 1,2,4,5-tetracyanobenzene (TETCB), 4,4′-dicyanobiphenyl (DCBP), 4,4″-dicyanoterphenyl (DCTP), and 2,6-dicyanopyridine (DCP) were purchased from Aldrich and used as received. Tris(4-cyanophenyl)amine (TCPA),[25] tris(4-cyanophenyl)benzene (TCPB),[26] tetra(4-cyanophenyl)adamantane (TCA),[27] 2,5-dicyanothiophene (DCT),[28] and 5,5′-dicyanobipyridine (DCBPY)[29] were prepared according to described procedures.

Characterization. Elemental analyses were obtained from a Vario El elemental analyzer. IR spectra were recorded on a Varian 1000-FTIR spectrometer equipped with an diamond ATR cell, and the samples were ground in a mortar prior to measurements. Nitrogen sorption measurements were collected on a Quantachrome Quadrasorb apparatus at 77 K. BET surface areas were determined over a P/P0 range as described.[30] The samples were degassed at 200 °C for 15 h before measurements. NLDFT pore size distributions were determined using the carbon/slit-cylindrical pore model of the Quadrawin software. A Nabertherm L3/11 oven was used as heating device. Transmission electron microscopy (TEM) was carried out with an Omega 912 (Carl Zeiss, Oberkochen, Germany). Scanning electron micrographs where acquired on a "Gemini" scanning electronic microscope (SEM). High-resolution TEM was performed on a Phillips CM 200 FEG electron microscope equipped with field emission gun. The acceleration voltage was set to 200 kV. The point resolution is 0.2 nm. Energy-dispersed X-ray spectra (EDX) were measured on the TEM with an EDXS spectrometer.

Synthesis of the Materials. In a typical experiment, the monomer (1.00 g) and the desired amount of $ZnCl_2$ were transferred into a quartz ampule (3 × 12 cm) under an inert atmosphere. The ampule was evacuated, sealed, and heated in 1 h to the desired temperature for the desired time. The ampule was then cooled down to room temperature and opened. **Caution:** for temperatures higher than 500 °C the ampules are under pressure, which is released during-opening. The reaction mixture was subsequently grounded and then washed thoroughly with water to remove most of the $ZnCl_2$. Further stirring in diluted HCl for 15 h was carried out to remove the residual salt. After this purification step, the resulting black powder was filtered, washed successively with water and THF, and dried in vacuum at 150 °C. Typical isolated yield: 90%. See Supporting Information Table S24 for elemental analyses of the materials.

Results and Discussion

A. Variation of Monomer Architecture. Besides the previously described 1,4-dicyanobenzene (pDCB) and the 4,4′-dicyanobiphenyl (DCBP), a number of monomers were employed for the dynamic salt melt condensation reaction. The choice of those monomers was essentially driven by easy availability, high thermal stability, and rigid monomer architecture (Scheme 2).

The conditions of polymerization and some properties of the resulting materials are summarized in Table 1 and compared to the data of the previously analyzed pDCB and DCBP. These two dinitriles feature a linear geometry that will stand as the reference monomers.

Different geometries of the monomer can be envisaged to tune the porous characteristics of the materials, as different positions of the nitrile moieties are expected to lead to different arrangements of the outcoming triazine scaffold. Therefore, it is relevant to compare dinitrile monomers that present different geometries, but featuring almost the same reactivity. The materials produced from mDCB are showing surface areas, porosities, and pore sizes (as determined by nitrogen adsorption−desorption measurements) very similar to the materials prepared from the linear pDCB in the same reaction conditions (as judged by comparison of entries 2/8, 4/9, and 6/10 in Table 1). It thus seems that changing the angle between the two nitriles does not drastically change the properties of the final material. Similarly, polymerization at 400 °C of the trinitrile TCB also produces a material with similar properties to the one obtained from pDCB in the same conditions (Table 1, entries 1/11), even if this monomer is a trisubstituted benzene ring that should give rise to a more dense network. Despite theses observations, the microstructure on the angstrom scale of the materials, which is not fully accessible by nitrogen sorption measurements, might present different characteristics, especially the presence of small micropores.

Tuning the pore size of the materials could also be accomplished by using monomers of different sizes. However,

Scheme 2. Monomers Employed for the Dynamic Nitrile Trimerization (DNT) Reaction

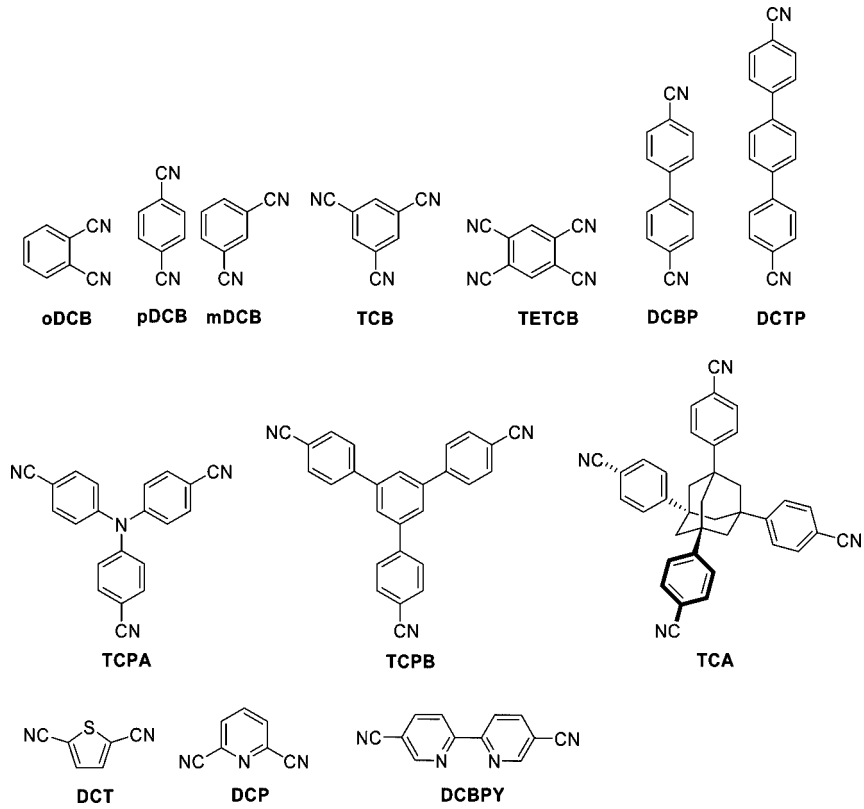

the polymerization of DCBP, which contain a biphenyl linker between the two nitriles, produces again a material quite similar to pDCB at 400 °C (Table 1, entries 2/15), especially when considering the pore sizes. We believe that the small variations found are not sufficient to illustrate a direct influence of the monomer size on the pore size distribution. As will be discussed later, due to the different reactivity of the DCBP monomer compared to the benzene analogues, experimental conditions such as temperature and concentration are much more critical for tuning the porous properties of this material.

Similar to DCBP, DCTP features a similar chemical structure with similar reactivity. Whereas the material obtained with 10 equiv of salt at 400 °C is almost only microporous (with an additional macroporosity), using 20 equiv of salt solvent has the influence to generate a mesopore system, from which the distribution is centered at ca. 8 nm. Both polymer scaffolds are highly porous, while the surface area increases with increasing the salt content, from 495 to 1900 $m^2\ g^{-1}$.

Also, polymerization of the large trigonal TCPB affords a porous material at 400 °C, with a surface area of 1200 $m^2\ g^{-1}$, being mainly microporous. Upon substitution of the central benzene ring by a nitrogen atom (TCPA), the material produced under standard conditions remains microporous, but with lower surface area.

Thus, changing the geometry and/or the size of the monomer does not allow a direct significant tuning of the pore size. We attribute this to the formation of interpenetrating scaffolded structures, as it is well-known from block copolymer mesophases, such as the gyroid structure or the interpenetrating double diamond motive.[31−33] This interpenetration can only be minimized by application of higher dilution.

Interestingly, using the much larger tetrahedral TCA featuring four nitrile moieties, a significant increase of the surface area can be observed. Here, values of 1500 $m^2\ g^{-1}$ are reached at 400 °C with only 4 equiv of salt. This goes well with our interpretation of interpenetration, as more massive units also can interpenetrate less. The adamantane moiety, otherwise thermally stable up to 450 °C, seems however to partly decompose at 400 °C in the presence of the Lewis acid, as detected by a high amount of gas produced during the polymerization. In turn, it was impossible to isolate a regular, 3-D crystalline material from this monomer. Interestingly, for TCA the surface area remains independent of the temperature and of the salt content, as an almost similar material is formed at 500 °C using 10 equiv of the salt.

B. Toward Functional Polymer Scaffolds. After having shown that the dynamic trimerization reaction can rather be generalized to a broader range of aromatic polynitriles, it was also tested if polymer functionality can be brought to the structure via the aromatic bridging unit. Again, a variety of monomers with ligating N- or S-functionality were employed as starting monomers.

As already mentioned before the N/C ratio of the monomer, and in turn the N/C ratio of the organic phase will determine its affinity to and miscibility with the salt phase and thus the porous characteristics of the resulting material.[34] A higher affinity between the monomer and the salt is achieved by adding nitrogen atoms to the bridging units. When the reaction is carried out at 400 °C with DCP, a moderate porosity is observed, and almost no porosity at all for the DCBPY (Table 1, entries 36 and 41). In both cases a fully condensed network is formed. The latter finding can be interpreted by the formation of rather stable complexes between the monomers and the salt, leading to dense metal−organic assemblies that prevent release of the solvent to allow pore formation. The strength of these complexes is given not only by the presence of the additional nitrogen atoms but also by their orientation supporting ligation. The materials contain also high amounts of residual salts (as determined by gravimetry) that cannot be removed even after extensive washing.

Table 1. Porous Characteristics of the Polymers Derived from Carbonitriles in Molten $ZnCl_2$

entry	monomer	temp (°C)	time (h)	$ZnCl_2$ (mol equiv)	S_{BET}[a] ($m^2\ g^{-1}$)	total pore vol[b] ($cm^3\ g^{-1}$)	av pore size[c] (nm)
1	pDCB	400	40	1.0	791	0.40	2.0
2	pDCB	400	40	5.0	920	0.47	2.0
3	pDCB	500	20	5.0	1600	1.00	2.5
4	pDCB	600	20	5.0	1750	2.09	3.6
5	pDCB	700	20	5.0	2530	2.26	3.6
6	pDCB	400/600	20/96	5.0	3270	2.4	2.9
7	oDCB	400	40	10	650	0.31	1.9
8	mDCB	400	40	5	810	0.39	1.9
9	mDCB	600	20	5	2100	2.06	3.9
10	mDCB	400/600	20/96	5	2810	2.61	3.7
11	TCB	400	40	1.5	730	0.39	2.1
12	TETCB	300	40	10	162	0.15	3.7
13	TETCB	400	40	10	40	0.18	17.7
14	DCBP	400	40	2	1150	0.57	2
15	DCBP	400	40	5	1140	0.64	2.2
16	DCBP	400	40	10	1710	1.2	2.8
17	MCBP	400	40	10	1130	1.5	5.3
18	DCBP	400	40	20	710	0.4	2.2
19	DCBP	600	20	2	1170	0.65	2.2
20	DCBP	600	20	5	1400	1.55	4.4
21	DCBP	600	20	10	1240	2.25	7.2
22	MCBP	600	20	10	675	1.67	10.0
23	BP	600	20	10	0	0	/
24	DCBP	600	20	15	1260	2.76	8.8
25	DCBP	600	20	20	1510	4.5	12.1
26	DCBP	400/600	20/20	5	1630	1.29	3.2
27	DCBP	400/600	20/20	10	1625	2.42	6.3
28	DCBP	400/600	20/20	20	1430	2.96	8.3
29	DCTP	400	40	10	495	0.97	7.8
30	DCTP	400	40	20	1900	2.25	4.7
31	TCPA	400	40	30	862	0.58	2.7
32	TCPB	400	40	30	1345	1.1	3.3
33	TCA	400	40	4	1618	1.26	3.1
34	TCA	500	20	10	1598	1.26	3.2
35	DCT	400	40	10	584	0.29	2.3
36	DCP	400	40	10	730	0.36	2.0
37	DCP	600	20	5	1095	0.56	2.0
38	DCP	400/600	20/20	5	2130	1.05	2.0
39	DCP/DCB	600	20	5	1375	0.82	2.4
40	DCP/DCBP	600	20	5	1910	1.34	2.8
41	DCBPY	400	40	10	0	0	/

[a] BET specific surface area. [b] At P/P0 = 0.99. [c] Determined from nonlocal density functional theory.

Scheme 3. Formation of a Phthalocyanine from 1,2-Dicyanobenzene

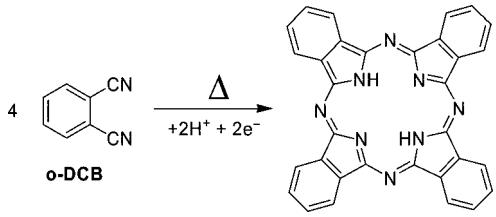

When a higher reaction temperature is used (600 °C, Table 1, entries 37 and 38), it was however possible to isolate a material with high porosity from DCP (up to 2130 $m^2\ g^{-1}$), virtually devoid of salt residue. Higher temperatures seems thus to help dissociation of the metal−organic complexes prior to consecutive reaction, thus leading to highly porous open structures with less optimal ligation motifs. For a further control of the functionality and pore structure, copolymerization of DCP with 1 equiv of DCB or DCBP was achieved at 600 °C (Table 1, entries 39 and 40). Whereas the DCP/DCB system produces a material mainly microporous, the copolymerization of DCP with DCBP allows the formation of an additional mesopore system.

According to the affinity of the DCP with $ZnCl_2$, it was anticipated that the resulting materials would feature excellent coordination abilities toward various transition metals. Indeed, already simple drawing of the motifs arising from the trimerization of the two nitriles of DCP point to the formation of bidentate or tridentate nitrogen ligands. Coordination study revealed that these materials are indeed behaving as very good solid state ligands toward several transition metals. This aspect will however be quantified in detail in an independent publication.

DCT allows the formation of a sulfur-rich material with a surface area of 580 $m^2\ g^{-1}$, even if weak degradation at 400 °C is leading to a partial depletion of the sulfur content. Elemental analysis on those structures showed indeed sulfur content of 15.6% (instead of the calculated 23.9% based on ideal stoichiometry). The observed incomplete combustion of the sample might however lead to underestimate the sulfur content, similarly to the general problem of nitrogen determination in all samples.

A special case of functionalization is found for dicyanobenzenes with the two nitriles in *ortho* arrangement. Indeed, aromatic *ortho* dinitriles are known to be precursors of phthalocyanines, the final functionality of which is based on the nitrile polymerization (Scheme 3).

This reaction occurs already at temperatures of about 180 °C in presence of metal salts. The polymerization of such monomers has already been carried out extensively, with the aim to prepare crystalline polyphthalocyanine materials.[35−37] *o*-Dicyanobenzenes might undergo three different reactions: the cyclization to phthalocyanine, the nitrile trimerization to triazines, and also linear polymerization leading to polyiminoisoin-

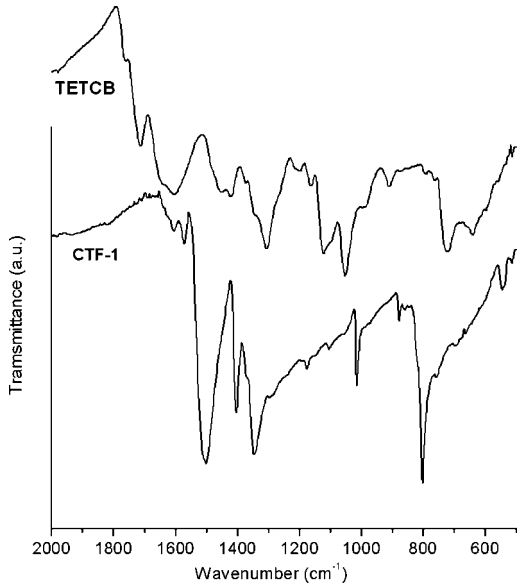

Figure 1. IR spectra of the material prepared from TETCB at 300 °C compared to that of CTF-1.

dolines. Heating *o*-DCB in the presence of 10 equiv of $ZnCl_2$ at 400 °C leads to an amorphous, black polymer network, free of soluble phthalocyanines. At an early stage of the reaction, a green coloration of the reaction medium however indicates the formation of these macrocycles. The porosity of the outcoming material is lower than for the other dicyanobenzenes. The surface area reaches 650 $m^2\ g^{-1}$ with an absolute pore volume of 0.3 $cm^3\ g^{-1}$. The lower porosities obtained here might arise from a higher density of the organic material due to the formation of a primary phthalocyanine intermediate. Indeed, when TETCB is used, which can potentially lead to a fully extended polyphthalocyanine network, materials with very low porosities are obtained. Again, energy-dispersed X-ray (EDX) measurements showed the presence of high amounts of residual $ZnCl_2$, which might be trapped in the form of Zn−phthalocyanine. Furthermore, this system exhibits a very different reactivity than the other dicyanobenzenes, as at 400 °C the material produced is almost only mesoporous. The IR spectrum of the material made from TETCB at 300 °C showed distinct absorption bands, different than the spectrum of a pure triazine based material (CTF-1)[13] (Figure 1).

The very strong bands characteristic of the triazine ring at 1350 and 1510 cm^{-1} are absent, whereas new bands are appearing at 1600, 1400, and 1100 cm^{-1}. These bands are also found in the spectrum of pure phthalocyanine. Therefore, it seems reasonable to assume that the material contains phthalocyanine rings in the network, which then undergo further polymerization.

It was thus shown that a variety of functionalities and coordination environments can be incorporated in the triazine scaffolds, leading to materials with great potentials for applications as catalytic supports.

C. Dynamic Self-Organization to Regular, "Crystalline" Porous Polymer Scaffolds. Most of the structures described up to now were disordered polymer scaffolds, i.e., networks with rather well-defined pores which however do not exhibit a long-range 3D-regular arrangement, giving rise to diffraction peaks in small-angle X-ray scattering. Until recently, it was supposed that the synthesis of such covalent "crystalline" organic polymer frameworks is impossible due to limitations of microreversibility associated with the creation of highly energetic covalent bonds. However, Yaghi et al. reported in 2005 the preparation of several covalent organic frameworks based on boroxine connectors that are accessed by the reversible condensation of boronic acids.[10,38] It was thus proven that by controlling the kinetics of reversible reactions, it is possible to obtain regular open covalent frameworks. Recently, we reported on a triazine-based material made from *p*-dicyanobenzene (CTF-1) which presents the same structural features as COF-1, but indeed with the advantage of the high chemical stability of a C−N-based polymer structure (Figure 2a).[13] Such a material could be prepared by the polymerization of *p*-dicyanobenzene with 1 equiv of $ZnCl_2$ at 400 °C for 40 h. A crystalline material was only obtained using 1 equiv of the salt.

Thus, small variations of the amount of salt close to this stoichiometry was carried out. It was found that the intensity of the diffraction peaks is dropping when the salt/monomer ratio is diverging from stoichiometry, as shown in Figure 2b. This is speaking for the coexistence of ordered and disordered domains at those compositions (0.6 or 1.4 equiv of salt).

To explain this feature, a templating effect of the salt can be envisaged, as this stoichiometry corresponds to complexes of the type $[ZnCl_2(RCN)_2]$. However, whatever the mechanism of the reaction is (an oxidative cyclization through a metallacycle intermediate or a nucleophilic substitution of a nitrile on a coordinated nitrile), a direct templating effect is highly improbable due to the difference of the symmetry of the reaction intermediates compared to the symmetry of the final triazine network; i.e., complexation does not prearrange the reactants into the right geometry.

Rather, an explanation taking into account the properties of the reaction medium seems more probable. Indeed, the 1:1 stoichiometry corresponds almost to the amount of salt just required to fill the pores of CTF-1 (1 g of CTF-1 has a pore volume of 0.4 cm^3 and the volume of 1 mol equiv of $ZnCl_2$ is 0.37 cm^3, using $\rho(ZnCl_2) = 2.907\ cm^3\ g^{-1}$).

D. Dynamic Self-Organization to Amorphous Porous Polymer Scaffolds: Influence of the Temperature and Concentration. The concentration of the monomer has a crucial influence on the properties of the materials. Indeed, a series of experiments carried out with pDCB using different amount of salt at fixed conditions (400 °C, 40 h) showed two different regimes (Figure 3a). For low amounts of salts (<1 equiv), the porosity is directly increasing with increasing the salt content. Thus, a minimum amount of salt is required to develop porosity (ca. 0.5 equiv), pointing to the fact that the salt is behaving as a porogen. When 1 equiv is used, as it was seen before, a special case is observed where the material present a periodic structure; i.e., the volume of salt corresponds to the pore volume of the material. For higher amounts of salt (>1 equiv), the variation of the porosity is this time rather weak; i.e., the amount of salt does not influence further the porous properties of the networks, and the pore size distribution remains almost constant (Figure 3b). However, in this regime, amorphous networks are produced, which are featuring porosities and surface areas closely related to the crystalline CTF-1 material. These observations tend to verify the assumption that the selective formation of CTF-1 arises from a specific concentration. To explain that high amounts of salt are hindering the formation of a crystalline material, it can be speculated that the excess of the salt interacts strongly with the growing cyclic oligomers (through Lewis acid−base interactions), thus preventing nucleation perpendicularly to the triazine planes.

Further investigations of the reaction conditions aimed to study the influence of the temperature. On going from 400 to 700 °C, it was observed that a well-defined mesoporosity was developed, with pore diameters of about 5 nm.[24] The same results are found for mDCB. This development of the mesoporosity leads to a drastic increase of the surface area (Figure 3c). This is a unique behavior, as usually heating a porous

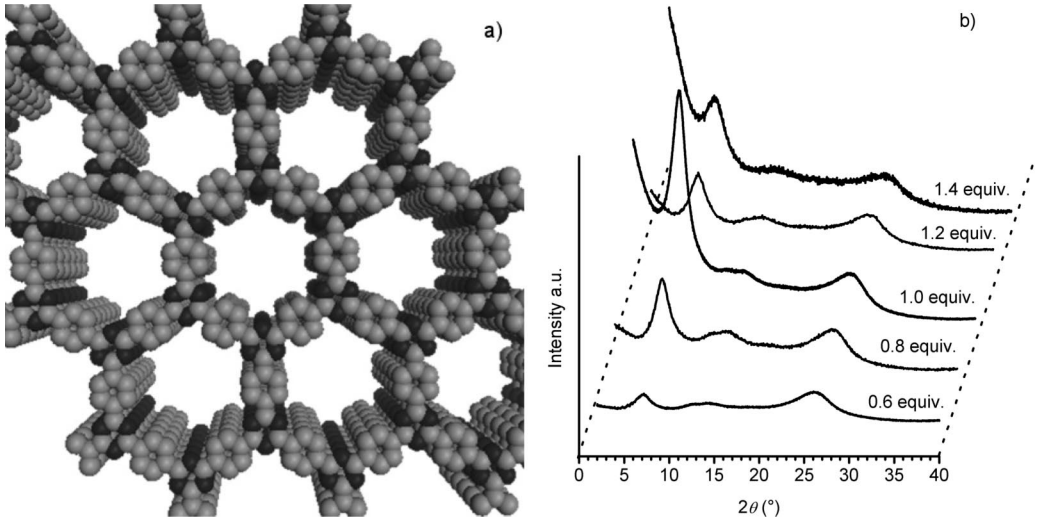

Figure 2. Representation of the idealized structure of CTF-1 (black: nitrogen; gray: carbon) (a) and XRD patterns of CTF-1 in function of the amount of zinc chloride (b).

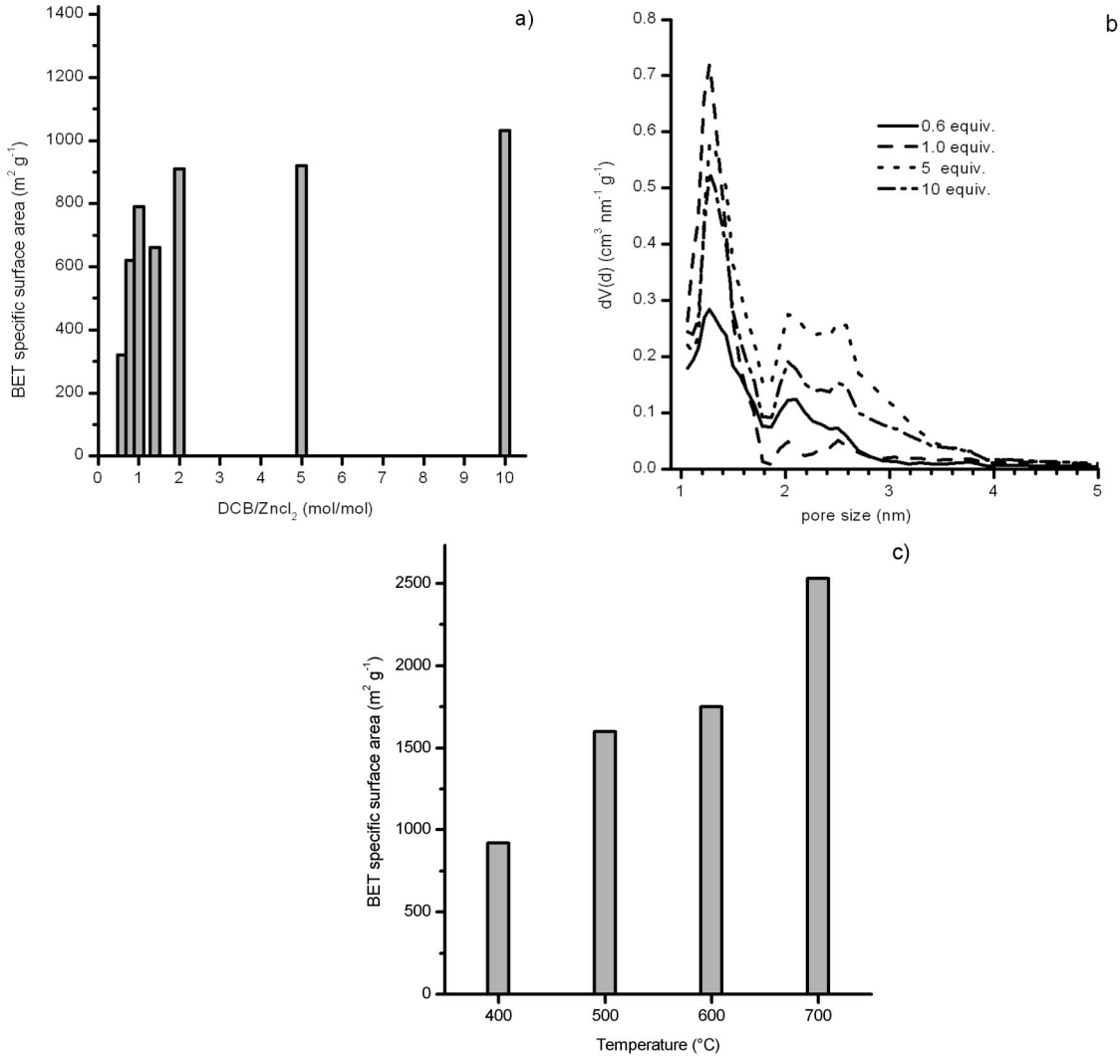

Figure 3. (a) Influence of the monomer concentration on surface area using pDCB as monomer (conditions: 400 °C, 40 h). (b) Pore size distribution in function of the concentration at 400 °C. (c) Influence of the temperature on the surface area.

material result in the slow disappearance of the pores due to capillarity and Ostwald ripening. High-resolution transmission electron micrographs have clearly confirmed the pseudo-hierarchical micro-mesoporosity.[24]

These results are pointing to another mode of self-organization of the system at higher temperatures. Careful analysis of chemical compositions and model experiments indicates that an additional reaction channel, irreversible C−C coupling

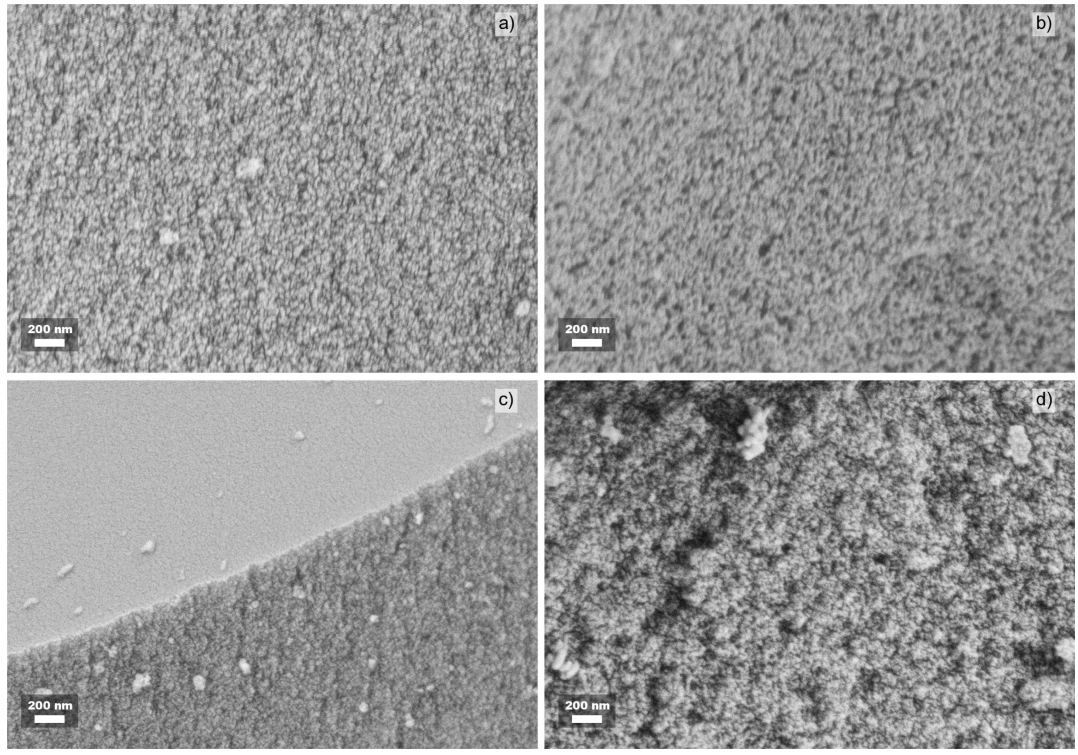

Figure 4. Scanning electron micrographs of (a) DCBP (5 equiv of $ZnCl_2$, 600 °C), (b) DCBP (20 equiv of $ZnCl_2$, 600 °C), (c) TCA (4 equiv of $ZnCl_2$, 400 °C), and (d) DCTP (10 equiv of $ZnCl_2$, 400 °C).

reactions, opens up,[24] which are well-known to occur for aromatic compounds under Lewis acidic conditions at these temperatures. To shed some light on this secondary self-organization, an additional experiment was carried out applying a high-temperature treatment to an already formed nonregular polytriazine network (Table 1, entry 6). In this case a material with properties similar to direct heating is obtained, while the pores are only slightly smaller and the surface area higher. Thus, it seems that the polymerization of nitriles and the reorganization of an already formed polytriazine network at 600 °C follow a quite similar pathway, in line with the fact that the nitrile trimerization equilibrium is the fastest reaction at this temperature. To explain the formation of mesopores, triazine retro-trimerization has to be taken into account. Opening triazine cross-links is leading to local expansions of the network. The formed CN moieties can then react also through irreversible C−C bond formations, trapping the locally expanded network under formation of larger pores. It has to be noted that the system is still polymeric and far from graphitization, which of course would also obstruct controlled mesopore formation.

The reorganization at 600 °C of the crystalline CTF-1 leads to an almost exclusively microporous material, reflecting the difficulty to rearrange triazine knots in the regular, packed arrangement. The product nevertheless still features a much higher surface area than the starting network. Thus, it appears that the treatment of CTF-1 at 600 °C follows an "exfoliation" pathway, as the final product is not X-ray crystalline anymore.

E. Nanoscale Phase Separation of Salt and Polymer: Toward Template Free Tailorable Mesoporosity. The generation of mesoporosity on the scale well beyond molecules and the "spontaneous" generation of interface area of course have to be based on a physicochemical driving phenomenon. It is close to assume that spinodal decomposition of the polymer/salt melt throughout structural rearrangement and denitrification of the polymer can be such a driver for self-organization. Spinodal decomposition of polymer mixtures is omnipresent for the generation of organized porosity[39,40] but leads to the formation of structures on the micrometer scale, and restrictions to the lower mesoscale are very rare.

Within the monomer variation presented in this work, it is straightforward to systematically vary the C/N ratio, thus controlling the affinity of the material for the salt phase and therewith the onset of the demixing by rational choice of the monomer, and thus the size of the mesopores can be tuned.

Indeed, such a variation is for instance possible with the DCBP system, where miscibility seems to be in a critical and therefore attractive range. When pure biphenyl is used (BP), a macro-phase separation is observed, resulting in a nonporous carbonaceous soot material. Using monocyanobiphenyl (MCBP), the resulting material presents a droplet-like morphology, the salt being the continuous phase, meaning that the two phases are demixing at rather early stages of the reaction. For DCBP, the organic polymer represents the continuous phase, and demixing only occurs throughout denitrification at elevated temperatures. In all cases, the materials are very homogeneous, and the pore sizes are quite well-defined, even if the distributions are slightly broadened when the size of the pores increases.

Similar morphologies are obtained for the DCTP and TCA featuring an even lower N/C ratio. In the case of DCTP, the material obtained at 400 °C with 10 equiv of $ZnCl_2$ presents a macroporosity in addition to the microporosity. However, using more salt (20 equiv) at the same temperature induces the formation of a mesopore system, without macroporosity. The rather homogeneous structure of the resulting porous scaffold, but also the increasing roughness with increasing mesopore size, is depicted with the scanning electron micrographs (SEM) (Figure 4).

The affinity of the monomer for the salt phase is therefore a crucial factor that can be used to control the hierarchical porosity of these materials. It has to be adequately balanced, as a too high or a too low affinity prevents the development of any useful porosity.

Conclusion

It was shown that the dynamic, reversible polymerization of a broad variety of aromatic nitriles results in polymer scaffolds or networks with controllable porosity and very high specific surface areas. Thus, the trimerization reaction toward triazines in $ZnCl_2$ salt melts at elevated temperatures could be generalized to many structurally different stiff monomers. The use of functional aromatic bridging units with pyridine, bipyridine, and thiophene functionality gave polymer scaffolds with the ability to coordinate metal salts in a stable porous polymer framework. These systems are promising as supports for metal organic catalysts. Application of higher temperatures while varying the monomer allowed clarifying the mechanism of scaffolds with extremely high surface areas and bimodal porosity. For given monomers with appropriate N/C ratio, phase separations can occur throughout condensation, resulting in a possible tuning of the mesopore size.

As the current systems can nicely compete in their sorption power and surface area with high-quality activated carbons, having the benefits of a very well-defined uniform polymer structure at the same time, we expect applications as sorption materials and as catalyst supports. Further work will be devoted to quantify the gas sorption characteristics and to analyze the performance as electrode materials for high-density batteries.

Acknowledgment. The ENERCHEM Project House of the Max Planck Society is gratefully acknowledged for financial support.

Supporting Information Available: EDX analysis, pore size distribution, and elemental analyses. This material is available free of charge via the Internet at http://pubs.acs.org.

References and Notes

(1) Hentze, H. P.; Antonietti, M. *Curr. Opin. Solid State Mater. Sci.* **2001**, *5*, 343–353.
(2) Davankov, V. A.; Tsyurupa, M. P. *Pure Appl. Chem.* **1989**, *61*, 1881–1888.
(3) Tsyurupa, M. P.; Davankov, V. A. *React. Funct. Polym.* **2006**, *66*, 768–779.
(4) Wood, C. D.; Tan, B.; Trewin, A.; Niu, H. J.; Bradshaw, D.; Rosseinsky, M. J.; Khimyak, Y. Z.; Campbell, N. L.; Kirk, R.; Stockel, E.; Cooper, A. I. *Chem. Mater.* **2007**, *19*, 2034–2048.
(5) Thomas, A.; Goettmann, F.; Antonietti, M. *Chem. Mater.* **2008**, *20*, 738–755.
(6) Cheetham, A. K.; Ferey, G.; Loiseau, T. *Angew. Chem., Int. Ed.* **1999**, *38*, 3268–3292.
(7) Lee, J.; Kim, J.; Hyeon, T. *Adv. Mater.* **2006**, *18*, 2073–2094.
(8) Ferey, G. *Chem. Soc. Rev.* **2008**, *37*, 191–214.
(9) Beck, J. S.; Vartuli, J. C.; Roth, W. J.; Leonowicz, M. E.; Kresge, C. T.; Schmitt, K. D.; Chu, C. T. W.; Olson, D. H.; Sheppard, E. W.; McCullen, S. B.; Higgins, J. B.; Schlenker, J. L. *J. Am. Chem. Soc.* **1992**, *114*, 10834–10843.
(10) Cote, A. P.; Benin, A. I.; Ockwig, N. W.; O'Keeffe, M.; Matzger, A. J.; Yaghi, O. M. *Science* **2005**, *310*, 1166–1170.
(11) Germain, J.; Frechet, J. M. J.; Svec, F. *J. Mater. Chem.* **2007**, *17*, 4989–4997.
(12) Jiang, J.-X.; Su, F.; Trewin, A.; Wood, C. D.; Campbell, N. L.; Niu, H.; Dickinson, C.; Ganin, A. Y.; Rosseinsky, M. J.; Khimyak, Y. Z.; Cooper, A. I. *Angew. Chem., Int. Ed.* **2007**, *46*, 8574–8578.
(13) Kuhn, P.; Antonietti, M.; Thomas, A. *Angew. Chem., Int. Ed.* **2008**, *47*, 3450–3453.
(14) McKeown, N. B.; Budd, P. M. *Chem. Soc. Rev.* **2006**, *35*, 675–683.
(15) Weber, J.; Su, Q.; Antonietti, M.; Thomas, A. *Macromol. Rapid Commun.* **2007**, *28*, 1871–1876.
(16) Weber, J.; Thomas, A. *J. Am. Chem. Soc.* **2008**, *130*, 6334.
(17) Rose, M.; Bohlmann, W.; Sabo, M.; Kaskel, S. *Chem. Commun.* **2008**, 2462–2464.
(18) Weber, J.; Antonietti, M.; Thomas, A. *Macromolecules* **2008**, *41*, 2880–2885.
(19) Goettmann, F.; Fischer, A.; Antonietti, M.; Thomas, A. *Chem. Commun.* **2006**, 4530–4532.
(20) Goettmann, F.; Fischer, A.; Antonietti, M.; Thomas, A. *Angew. Chem., Int. Ed.* **2006**, *45*, 4467–4471.
(21) Groenewolt, M.; Antonietti, M. *Adv. Mater.* **2005**, *17*, 1789.
(22) Johns, I. B.; Smith, J. O.; McElhill, E. A. *Ind. Eng. Chem. Prod. Res. Dev.* **1962**, *1*, 277–281.
(23) Miller, G. H. U.S. Patent 3,775,380, **1973**.
(24) Kuhn, P.; Forget, A.; Su, D.; Thomas, A.; Antonietti, M. *J. Am. Chem. Soc.* **2008**, *130*, 13333–13337.
(25) Gorvin, J. H. *J. Chem. Soc., Perkin Trans. 1* **1988**, 1331–1335.
(26) Wang, Z. Y.; Zha, Z. G.; Zhang, J. H.; Wu, J. H. *Chin. Chem. Lett.* **2003**, *14*, 13–16.
(27) Shen, D.-M.; Chapman, O. L.; Lin, L.; Ortiz, R. U.S. Patent 5,347,063, **1994**.
(28) Paulmier, C.; Morel, J.; Pastour, P.; Semard, D. *Bull. Soc. Chim. Fr.* **1969**, 2511–2519.
(29) Veauthier, J. M.; Carlson, C. N.; Collis, G. E.; Kiplinger, J. L.; John, K. D. *Synthesis* **2005**, 2683–2686.
(30) Walton, K. S.; Snurr, R. Q. *J. Am. Chem. Soc.* **2007**, *129*, 8552–8556.
(31) Winey, K. I.; Thomas, E. L.; Fetters, L. J. *Macromolecules* **1992**, *25*, 422–428.
(32) Hajduk, D. A.; Harper, P. E.; Gruner, S. M.; Honeker, C. C.; Kim, G.; Thomas, E. L.; Fetters, L. J. *Macromolecules* **1994**, *27*, 4063–4075.
(33) Antonietti, M.; Caruso, R. A.; Goltner, C. G.; Weissenberger, M. C. *Macromolecules* **1999**, *32*, 1383–1389.
(34) Kuhn, P.; Forget, A.; Hartmann, J.; Thomas, A.; Antonietti, M. *Adv. Mater.* **2008**, in press.
(35) Yanagi, H.; Wada, M.; Ueda, Y.; Ashida, M.; Wohrle, D. *Macromol. Chem. Phys.* **1992**, *193*, 1903–1911.
(36) Yakushi, K.; Shirotani, I.; Khairullin, I. I.; Nakazawa, Y.; Kanoda, K.; Kosugi, N.; Takeda, S. *Synth. Met.* **1995**, *71*, 2287–2288.
(37) Lin, J. W. P.; Dudek, L. P. *J. Polym. Sci., Part A: Polym. Chem.* **1985**, *23*, 1579–1587.
(38) El-Kaderi, H. M.; Hunt, J. R.; Mendoza-Cortes, J. L.; Cote, A. P.; Taylor, R. E.; O'Keeffe, M.; Yaghi, O. M. *Science* **2007**, *316*, 268–272.
(39) Steinhart, M.; Wehrspohn, R. B.; Gosele, U.; Wendorff, J. H. *Angew. Chem., Int. Ed.* **2004**, *43*, 1334–1344.
(40) Binder, K. *J. Non-Equilib. Thermodyn.* **1998**, *23*, 1–44.

MA802322J